OLD DOMINION UNIVERSITY RESEARCH FOUNDATION

DEPARTMENT OF MATHEMATICAL SCIENCES
SCHOOL OF SCIENCES AND HEALTH PROFESSIONS
OLD DOMINION UNIVERSITY
NORFOLK, VIRGINIA

(NASA-CR-169028) MODELING OF THIN-FILM GaAs GROWTH Progress Report, 30 Jan. 1981 - 16 Jun. 1982 (Old Dominion Univ., Norfolk, Va.) 20 p HC A02/MF A01 CSCL 20B N82-27159
Unclas
G3/76 28097

MODELING OF THIN-FILM GaAs GROWTH

By

John H. Heinbockel, Principal Investigator

Progress Report
For the period January 30, 1981 to June 16, 1982

Prepared for the
National Aeronautics and Space Administration
Langley Research Center
Hampton, Virginia 23665

Under
Research Grant NAG1-148
Ronald A. Outlaw, Technical Monitor
Space Systems Division

June 1982

DEPARTMENT OF MATHEMATICAL SCIENCES
SCHOOL OF SCIENCES AND HEALTH PROFESSIONS
OLD DOMINION UNIVERSITY
NORFOLK, VIRGINIA

MODELING OF THIN-FILM GaAs GROWTH

By

John H. Heinbockel, Principal Investigator

Progress Report
For the period January 30, 1981 to June 16, 1982

Prepared for the
National Aeronautics and Space Administration
Langley Research Center
Hampton, Virginia 23665

Under
Research Grant NAG1-148
Ronald A. Outlaw, Technical Monitor
Space Systems Division

Submitted by the
Old Dominion University Research Foundation
P.O. Box 6369
Norfolk, Virginia 23508-0369

June 1982

MODELING OF THIN-FILM GaAs GROWTH

By

John H. Heinbockel*

INTRODUCTION

The Solid-on-Solid (SOS) model of crystal growth (ref. 1) is represented by a rectangular array of integers where each integer represents the number of adatoms in a column perpendicular to some reference frame. The adatoms can represent atoms or molecules that are being stacked. Figure 1 illustrates the surface adatoms that are at the tops of their columns. It is assumed that an adatom event of adsorption or desorption can only occur at the top of a column.

We are concerned with constructing a model of crystal growth that takes into account the processes of nucleation on the growing surface as well as considering the processes of surface migration and desorption of adatoms.

In the SOS model the columns are constructed upon an M × M-square array by randomly placing adatoms upon the array and allowing these randomly deposited adatoms to either condense, evaporate, or migrate. The SOS model can be described as an array of interacting columns of varying integer heights. The surface adatoms, being at the tops of columns, are allowed to migrate, remain stationary, or evaporate as is dictated by a set of rules which will be described presently.

The term "epitaxy" means "an arrangement" and is used to denote the growth of one substance upon the crystal surface of a foreign substance. The term "autoepitaxy" is the oriented growth of a substance onto itself and "hetroepitaxy" is used for the growth of one material upon the surface of a different material. Obviously, hetroepitaxy becomes autoepitaxy after one layer of adatoms has been deposited over the growing surface. We use the SOS method to simulate epitaxial growth of crystals.

*Professor, Department of Mathematical Sciences, Old Dominion University, Norfolk, Virginia 23508.

LIST OF SYMBOLS

i,j	site numbers
M	size of square array
$U_o = U_o(i,j)$	potential at site (i,j)
$\phi 0, \phi 1, \phi 2, \phi 3$	potential energy changes
w_i, $i = 1, \ldots, 8$	potential energy changes
$E(i,j)$	random energy
Δt	time interval
$U = U(i,j)$	total energy at site (i,j)
U_e	evaporation potential
U_m	migration potential
E	energy
K	Boltzmann constant
T	temperature
$f(E)$	Boltzmann distribution
(100) (110) (111)	crystal orientations
α_2, α_3	scale factors
ξ	crystal orientation factor
$U_{ks}^{(1)}$, $U_{ks}^{(2)}$	kink site potentials
ΔHevap	heat of evaporation
N_e, N_m, N_e	fraction of adatoms evaporating, migrating or remaining localized
Γ_{ij}	position factor

POTENTIAL ENERGY OF ADATOMS

The rules by which the columns of the SOS model interacted were governed by the following ideas relating to the potential energy and potential energy changes associated with the adsorption, migration, or desorption of adatoms from an arbitrary row i and column j of an $M \times M$ array. Energies associated with an arbitrary site (i,j) were defined as follows: $U_0 = U_0(i,j)$--the potential energy at a site because of surface bonding and crystal structure; ϕ_0--the potential energy change at site (i,j) because of the deposition of an adatom (assumed the same for all sites); $-W_i(i = 1, \ldots, 8)$--the potential energy changes at neighboring sites when an adatom is deposited at site (i,j); $E(i,j)$--the random surface energy associated with site (i,j) and time interval Δt; $U(i,j) = U_0(i,j) + E(i,j)$--the total energy associated with site (i,j) during the time interval Δt; U_e--the evaporation potential; and U_m--the migration potential. All of the above energies were measured in electron volts.

We developed a Monte Carlo computer simulation of crystal growth (refs. 2, 3, 4, and 5) by developing rules that determined the SOS kinetics of condensation evaporation or surface migration of adatoms. These rules led to a consistent and physically reasonable description of the fundamentals associated with crystal growth. We first considered the adsorption of a thermally accommodated adatom onto the surface at some general site where the potential at this site was changed and, simultaneously, potential energy changes at all of the neighboring sites occurred. In Table 1 the potential energy changes are depicted by the mnemonic mask. The center of this mask is placed over the site (i,j) to illustrate the changes to be made in the potential at the central site as well as the potential changes in the surrounding neighboring sites.

The potential changes in the case of desorption of an adatom from the central site are again depicted with the mask of Table 1, with the opposite signs on the potential changes. The case of surface migration was treated as a desorption from a site (i,j) followed by an adsorption at a nearest neighbor location, together with the correct potential mask changes associated with each process. The nearest neighbor migration site was determined by a random walk to one of the unoccupied nearest neighbor sites.

Table 1. Potential energy changes associated with central site (i,j) and neighbor sites due to deposition of an adatom.

$-w_7 = -w_7(i-1,j-1)$	$-w_8 = -w_8(i-1,j)$	$-w_1 = -w_1(i-1,j+1)$
$-w_6 = -w_6(i,j-1)$	$\phi_0 = \phi_0(i,j)$	$-w_2 = -w_2(i,j+1)$
$-w_5 = -w_5(i+1,J-1)$	$-w_4 = -w_4(i+1,j)$	$-w_3 = -w_3(i+1,j+1)$

The Monte Carlo simulation of crystal growth involved a random deposition of thermally accommodated surface adatoms during a time interval Δt. These deposited adatoms changed the potential energies at the random surface sites under consideration. The values assigned to the central potential change ϕ_0 and neighboring potential changes $-w_i$, $i = 1, \ldots, 8$ dictated the new potential energy values when an adatom was deposited or removed from a site. In this way each surface site had an energy barrier to translation or evaporation, represented by a potential well. We assumed that the thermally accommodated adatoms had a surface energy distribution described by the Boltzmann distribution

$$f(E) = \frac{1}{KT} \exp\left(\frac{-E}{KT}\right), \quad E > 0 \tag{1}$$

which has a mean energy of KT.

During each time interval Δt, the Boltzmann distribution was used to assign a random energy $E(i,j)$ to each of the surface adatoms. We let

$$U(i,j) = U_o(i,j) + E(i,j) \tag{2}$$

denote the total energy possessed by a surface adatom at a site (i,j) during this time interval. This total energy is the sum of the potential energy U_o due to the lattice structure and a random energy E from the Boltzmann distribution which characterizes the random surface energy. When U was less than some material-dependent migration level U_m, the adatom remained stationary at the surface site. If $U_m < U < U_e$, surface migration by random walk was allowed to occur. If U was greater than the evaporation potential U_e, the adatom was removed from the site.

The rate of impingement of adatoms upon the surface was independent of the surface configuration. The rates associated with the evaporation and migration of adatoms depended upon the potential barriers U_e and U_m and also upon the values assigned to the potential changes Φ_o and $-w_i$, $(i = 1, \ldots, 8)$. These later potential changes had to take into account the type of crystal structure and orientation of the growth we were trying to simulate with the SOS model. In Figure 2(a), for growth on the (100) face, we set up a correspondence between the central site, the nearest neighbor potentials ϕ, second nearest neighbor potentials ϕ_2, and the adatom potential changes for the mask in Table 1 (e.g., $w_1 = \phi_2$, $w_2 = \phi_1$). In a similar manner we were able to set up the correspondences illustrated in Figure 2(b) and (c) for the (111) and (110) orientations. In Table 2, we selected the relation between the neighbor potentials ϕ_0, ϕ_1, ϕ_2, ϕ_3 in such a way that when the first level of adatoms covered the surface, the potential distribution returned to its original value. By simply adding adatoms to the surface it was readily verified that the potential changes, assigned to the mask, had to adhere to the rules given in Table 2. In these rules, a negative sign denotes an attractive potential and after one complete layer of adatoms is deposited, the potential energy values at each site will return to their initial values.

We let ϕ_1 denote the change in the nearest neighbor potentials due to the addition of an adatom to the surface and let ϕ_2, ϕ_3 denote the second and third nearest neighbor potential changes. We assumed that $\phi_2 = \alpha_2\phi_1$ and $\phi_3 = \alpha_3\phi_1$ where α_2, α_3 are scale factors which are less than one. This allowed us to define the crystal orientation factor ξ as

$$\xi = \begin{cases} 2 + 2\alpha_2 & , \quad (100) \\ 3 + \alpha_2 & , \quad (111) \\ 1 + \alpha_2 + 2\alpha_3, & \quad (110) \end{cases} \tag{3}$$

which takes into account the different crystal orientations. We also defined the kink site potentials before $U_{ks}^{(1)}$ and after $U_{ks}^{(2)}$ and the capture of an adatom as $U_{ks}^{(1)} = U_o - \xi\phi_1$, $U_{ks}^{(2)} = U_o + \xi\phi_1$. (Note that $\Phi_o = 2\xi\Phi_1$.)

Table 2. Potential changes for addition of an adatom to an arbitrary site.

Crystal Face	Relation Between Neighbor Potentials	Potential Changes for Addition to Arbitrary Site I	Distances to Neighboring Sites
		$\begin{bmatrix} -\omega_7 & -\omega_8 & -\omega_1 \\ -\omega_6 & \phi_0 & -\omega_2 \\ -\omega_5 & -\omega_4 & -\omega_3 \end{bmatrix}$	
(100)	$\phi_0 = 4\phi_1 + 4\phi_2$	$\begin{bmatrix} -\phi_2 & -\phi_1 & -\phi_2 \\ -\phi_1 & -\phi_0 & -\phi_1 \\ -\phi_2 & -\phi_1 & -\phi_2 \end{bmatrix}$	a_0; $\frac{\sqrt{2}}{2}a_0$
(111)	$\phi_0 = 6\phi_1 + 2\phi_2$	$\begin{bmatrix} -\phi_1 & -\phi_1 & -\phi_2 \\ -\phi_1 & \phi_0 & -\phi_1 \\ -\phi_2 & -\phi_1 & -\phi_1 \end{bmatrix}$	$\sqrt{\frac{3}{2}}\,a_0$; $\frac{\sqrt{2}}{2}a_0$; $\frac{\sqrt{2}}{2}a_0$
(110)	$\phi_0 = 2\phi_1 + 2\phi_2 + 4\phi_3$	$\begin{bmatrix} -\phi_3 & -\phi_2 & -\phi_3 \\ -\phi_1 & \phi_0 & -\phi_1 \\ -\phi_3 & -\phi_2 & -\phi_3 \end{bmatrix}$	a_0; $\sqrt{\frac{3}{2}}\,a_0$; $\frac{\sqrt{2}}{2}a_0$

THE SIMULATION MODEL AND PARAMETERS

A flow chart of the simulation model is illustrated in Figure 3. The model is simple and presents an alternative viewpoint for the interaction of surface molecules: An assumed impingement rate dictates the number of adatoms arriving on the surface during a time interval Δt. Each of these adatoms are added to the surface at random sites and the potentials at each of these sites and neighboring sites are adjusted. If the Δt time interval is so small that no adatoms arrive on the surface, then every surface adatom can still be assigned a random energy from the Boltzmann distribution and surface interactions can be taken into account. We continued scanning the surface each Δt time interval until enough time accumulated for the addition of another adatom.

The model allows for various assumptions to be made about the interaction of potentials and assignment of potential values. We let $U_e = 0$ denote the evaporation level, then $\Delta U_e = U_e - U_o$ represented the desorption energy ΔHevap. The activation energy for migration of adatoms in a flat surface was $\Delta U_m = U_m - U_o$. The various potentials are illustrated in the Figure 4. The values assigned to U_m and U_o greatly affected the model behavior. For example, the Boltzmann distribution is illustrated in Figure 5, where nominal values of ΔU_m and ΔU_e are illustrated. The number of surface adatoms with a statistical surface energy less than ΔU_m is proportional to the area under the probability density curve which is given by $N_\ell = 1 - \exp(-\Delta U_m/KT)$. The number of adatoms that escaped from the surface is proportional to $N_e = \exp(-\Delta U_e/KT)$ and the number of adatoms that migrated is proportional to the area $N_m = 1 - N_\ell - N_e$. Letting $\alpha = \Delta U_m/\Delta U_e$, Figure 6 was constructed which illustrates the migration effect as α decreases.

The values of ϕ_0, ϕ_1, ϕ_2, ϕ_3 which denote the potential energy changes at a central site (i,j) and nearest neighbor sites can be different for the substrate and the growing material. For the substrate material we could use the depth of the surface potentials and migration levels to stimulate a variety of surface morphologies. In this model we envisioned a flat substrate as a periodic lattice structure 20-x-20 square where each lattice is a potential well. The substrate can vary from flat to rough and the potentials adjusted to reflect various surface preparations. For an ideally flat substrate we assumed that the depths of the potential wells were uniform, given by U_{os}. After one layer of growing material covered the surface, the potentials at each site were assumed to convert to the autoepitaxy potentials U_o. In order to make this transition we assumed that $\phi_o = \sum_{i=1}^{8} w_i + (U_o - U_{os})\Gamma_{ij}$ where Γ_{ij} is zero if the height h_{ij} at position (ij) is greater than or equal to one and Γ_{ij} is one in the case where h_{ij} is zero. Thus, if an adatom was deposited at a first layer site (i,j) we adjusted the potential at this site by the relation by $U_o - U_{os}$ in addition to the mask potential changes as this produced the desired change that hetroepitaxy produces in the potential at the surface site.

Nucleation on the substrate was controlled by the values assigned to ΔU_e, ΔU_m, and ϕ_o. For large values of ΔU_m there were deep potential wells that captured all thermally accommodated adatoms. For small ΔU_m values there was an increase in surface migration and a decrease in the number of adatoms that remained localized. This increased the probability of an adatom combining with other adatoms to form a critical cluster. Then growth was characterized by the lateral motion of adatoms and their addition to the steps of clusters that produced the lateral growth.

Various potentials were proposed for the addition of an adatom to the surface (refs. 6 and 7):

Buckingham Potential $\quad E = He^{-Br} - \frac{\lambda_0}{r^6} - \frac{\lambda_1}{r^8}$

Modified Buckingham Potential $\quad E = \left[\frac{6}{\alpha} e^{\alpha\left(1 - \frac{r}{rm}\right)} - \left(\frac{rm}{r}\right)^{6}\right] \frac{\varepsilon}{1 - \frac{6}{\alpha}}$

Lennard-Jones (Mie Potential) $\quad E = \frac{\lambda n}{r^n} - \frac{\lambda m}{r^m}$

Morse Potential $\quad E = De^{-2\alpha(r - r_o)} - De^{-(r - r_o)}$

Born-Mayer Potential $\quad E = Ae^{-Br}$

These potentials reflect the vertical effect of potential change. For the lateral interaction between potentials and resultant changes (ref. 8), we find:

Kiselev Potential $E = E_o - NCf(r)$

where E_o is interaction at zero coverage, C is dispersion constant, N is the number of nearest neighbors at half a monolayer coverage and r is mean distance between molecules.

Output from the computer program can be graphic as illustrated in the Figure 7 or quantitative.

QUANTITATIVE MEASURES OF CRYSTAL GROWTH AND PARAMETERS OF MODEL

Measures of Crystal Growth

1. Growth rate of crystal
2. Critical clusters
   a. size
   b. shape
   c. density
   vs. time or deposition rate
3. Surface diffusion (mobility)
4. Condensation rate
5. Evaporation rate
6. Rate of nucleation
7. Other characteristics

Parameters of Model

1. Deposition rate of adatoms
2. Potential changes ϕ_0, ϕ_1, ϕ_2, ϕ_3
3. Mean U_0 and standard deviation σ_0 associated with normal distribution $N(U_0, \sigma_0)$ of surface potentials (initially $U_0 = 0$)
4. Traps in Surface
5. Temperature of substrate
6. Number of migration scans (time Δt)
7. Crystal orientation
8. Substrate and growing potentials can be different
9. Mean U_m and standard deviation σ_m of migration levels associated with normal distribution $N(U_m, \sigma_m)$
10. Initial substrate geometry and potentials
11. Assumptions in regard to retention of incident energy

$$E_{random} = \underset{\text{(Surface Energy)}}{E_{Boltzmann}} + \underset{\text{(Kinetic Energy of Incident Adatom)}}{E_{Retention}}$$

NOMINAL VALUES FOR POTENTIAL ENERGIES FOR GERMANIUM IN EV (1 EV = 23 KCAL/MOLE)*

$\Delta Hevap = 3.87$ ev

$\Delta Hads = .86$ ev	Ge on C_aF_2	$Q_d = .52$ ev	G_e on C_aF_2
$\Delta Hads = .55$ ev	Ge on graphite	$Q_d = .32$ ev	G_e on graphite
$\Delta Hads = .60$ ev	Ge on carbon	$Q_d = .35$ ev	G_e on carbon
$\Delta Hads = 1.6$ ev	Ge on W	$Q_d = .75$ ev	G_e on G_e

* See ref. 9.

REFERENCES

1. Weeks, J.D. and Gilmer, G.H.: "Dynamics of Crystal Growth." Advances in Chemical Physics, Vol. 40, John Wiley & Sons, 1979.

2. Abraham, F.F. and White, G.M.: "Computer Simulation of Vapor Deposition on Two-Dimensional Lattices." J. Appl. Phys., Vol. 41, No. 4, March 15, 1970, pp. 1841-1849.

3. Gilmer, G.H.: "Simulation of Crystal Growth from the Vapor." Arsenault, R.J., Beeler, J.R. Jr., and Simmons, J.A., eds., Proceedings, International Conference on Computer Simulation for Materials Applications, April 19-26, 1976. National Bureau of Standards (Gaithersburg, MD).

4. Gilmer, G.H.: "Computer Models of Crystal Growth." <u>Science</u>, Vol. 28, 1980, pp. 355-363.

5. Gilmer, G.H. and Bennema, P.: "Simulation of Crystal Growth with Surface Diffusion." J. Appl. Phys., Vol. 43, No. 4, April 1972, pp. 1347-1360.

6. Lewis, B. and Anderson, J.C.: <u>Nucleation and Growth of Thin Films</u>. New York: Academic Press, 1978.

7. Torrens, I.M.: <u>Interatomic Potentials</u>. New York: Academic Press, 1978.

8. Young, D.M. and Crowell, A.D.: <u>Physical Absorption of Gases</u>. Butterworths, 1962.

9. Krikorian, E. and Sneed, R.J.: "Nucleation, Growth, and Transformation of Amorphous and Crystalline Solids Condensing From the Gas Phase." Astrophysics and Space Science, Vol. 65, 1979, pp. 129-154.

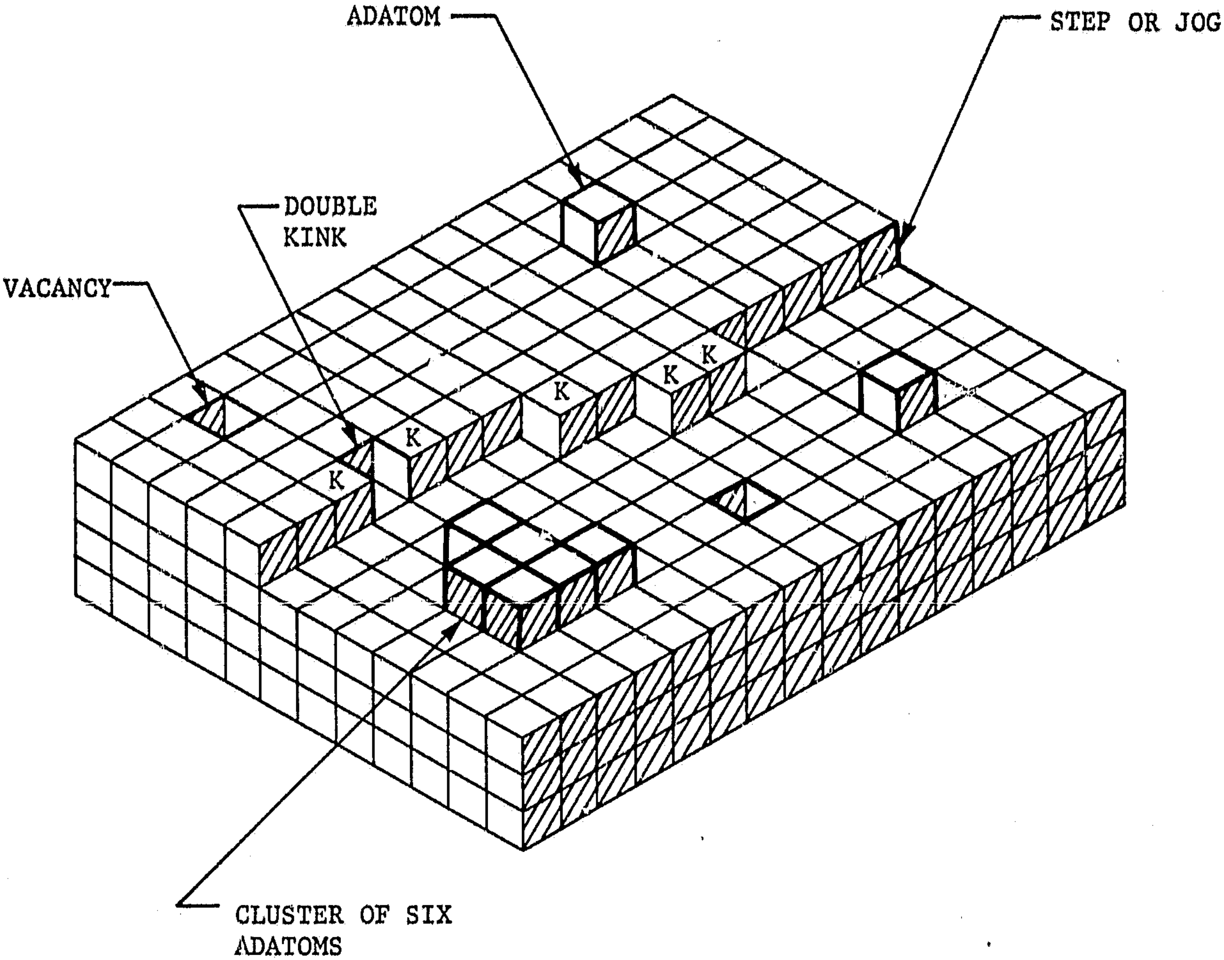

Figure 1. SOS model for crystal growth.

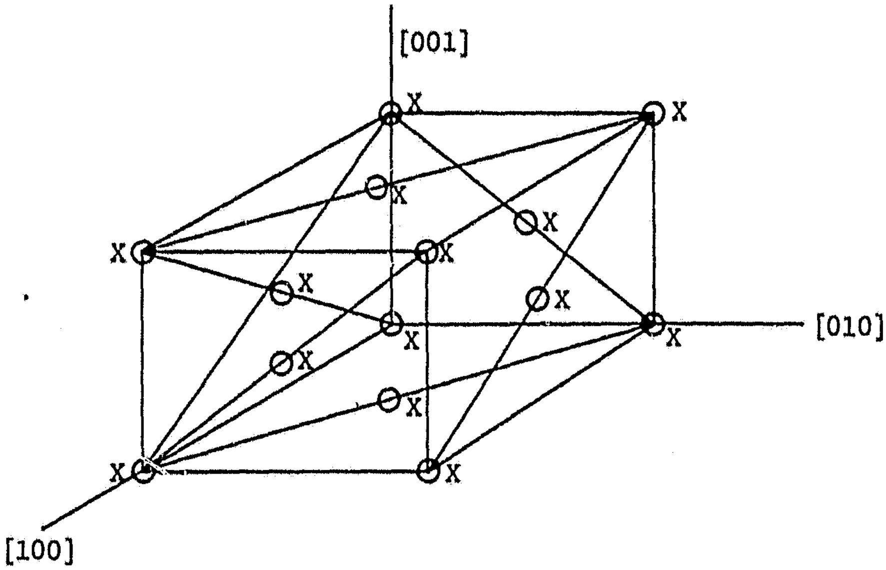

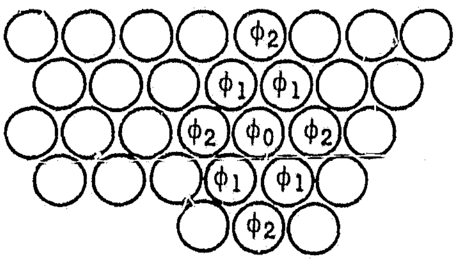

IN TERMS OF SOS MODEL

$-\phi_2$	$-\phi_1$	$-\phi_2$
$-\phi_1$	ϕ_0	$-\phi_1$
$-\phi_2$	$-\phi_1$	$-\phi_2$

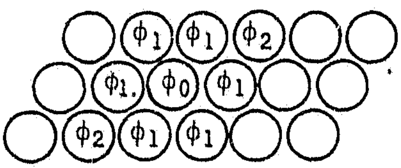

IN TERMS OF SOS MODEL

$-\phi_1$	$-\phi_1$	$-\phi_2$
$-\phi_1$	ϕ_0	$-\phi_1$
$-\phi_2$	$-\phi_1$	$-\phi_1$

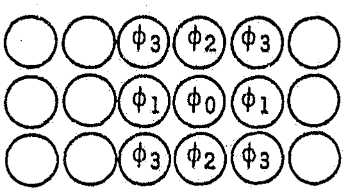

IN TERMS OF SOS MODEL

$-\phi_3$	$-\phi_2$	$-\phi_3$
$-\phi_1$	ϕ_0	$-\phi_1$
$-\phi_3$	$-\phi_2$	$-\phi_3$

Figure 2. FCC model and potential changes associated with different crystal orientations.

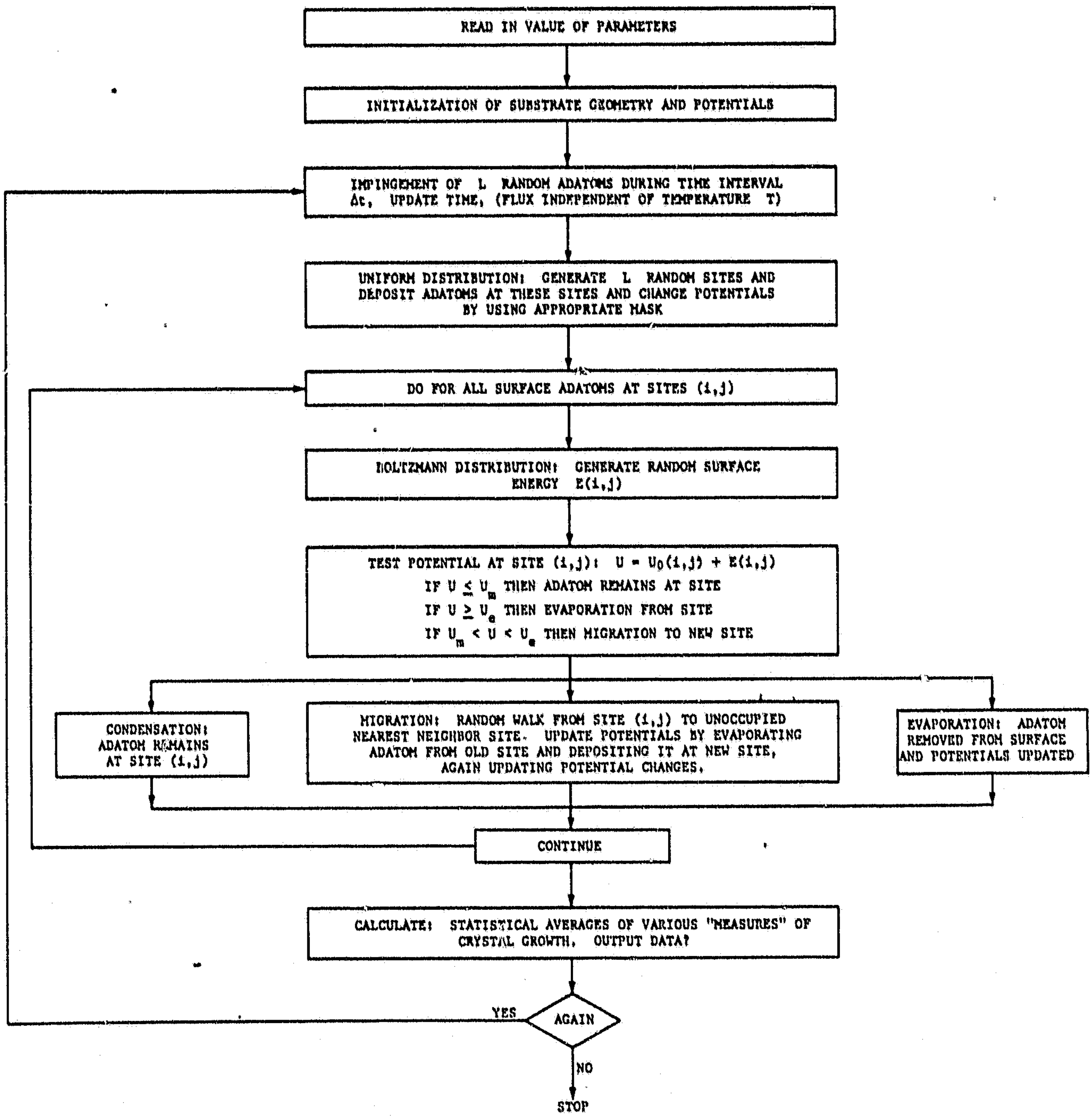

Figure 3. Flow chart of simulation model.

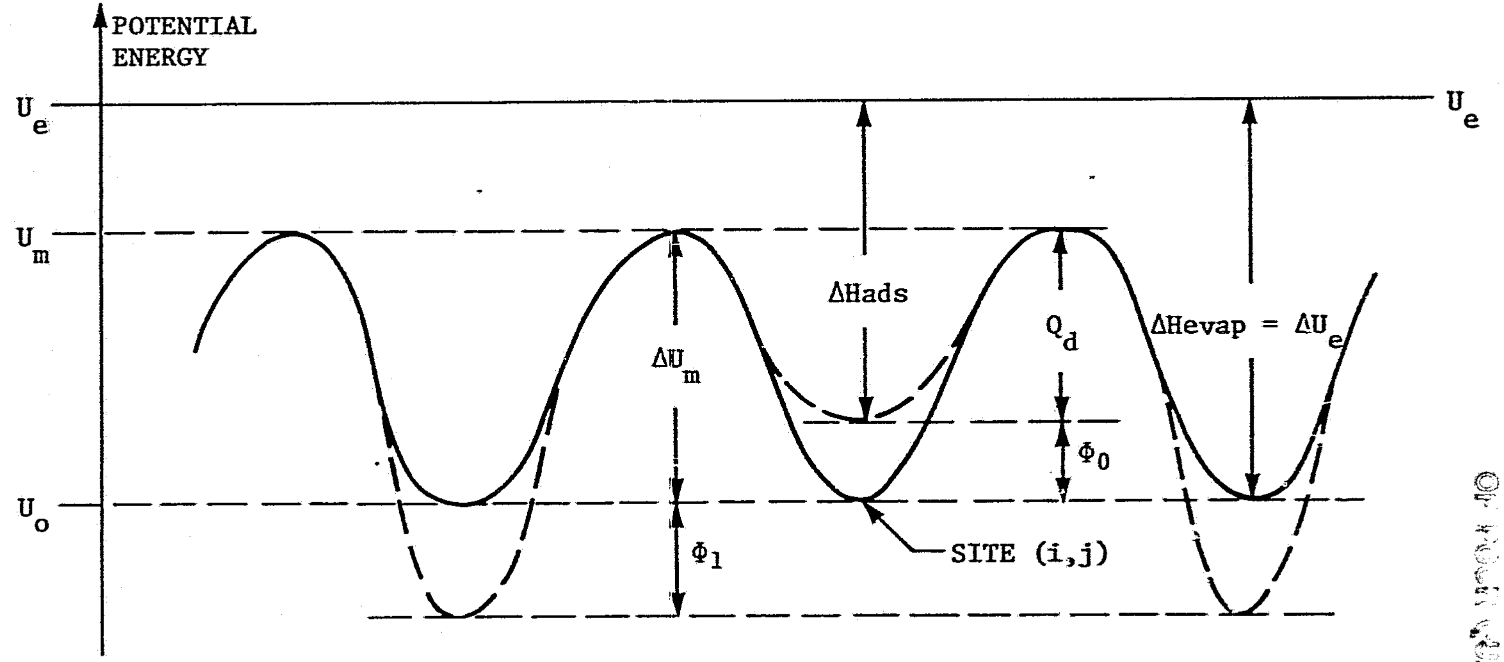

ΔHads = HEAT OF ADSORPTION FOR SINGLE ADATOM

ΔHevap = HEAT OF EVAPORATION

U_e = EVAPORATION BARRIER

U_m = MIGRATION BARRIER

U_0 = −ΔHevap = NOMINAL VALUE FOR POTENTIAL UNIFORM SURFACE

Φ_0 = ΔHevap − ΔHads = POTENTIAL CHANGE DUE TO ADDITION OF ADATOM AT SITE (i,j)

ϕ_1 = NEAREST NEIGHBOR POTENTIAL CHANGE

ϕ_2 = SECOND NEAREST NEIGHBOR POTENTIAL CHANGE

Q_d = DIFFUSION ACTIVATION ENERGY

Figure 4. Potentials for uniform flat surface (solid line) and potential after adatom has been added to site (i,j) (dashed line) together with energy barrier nomenclature.

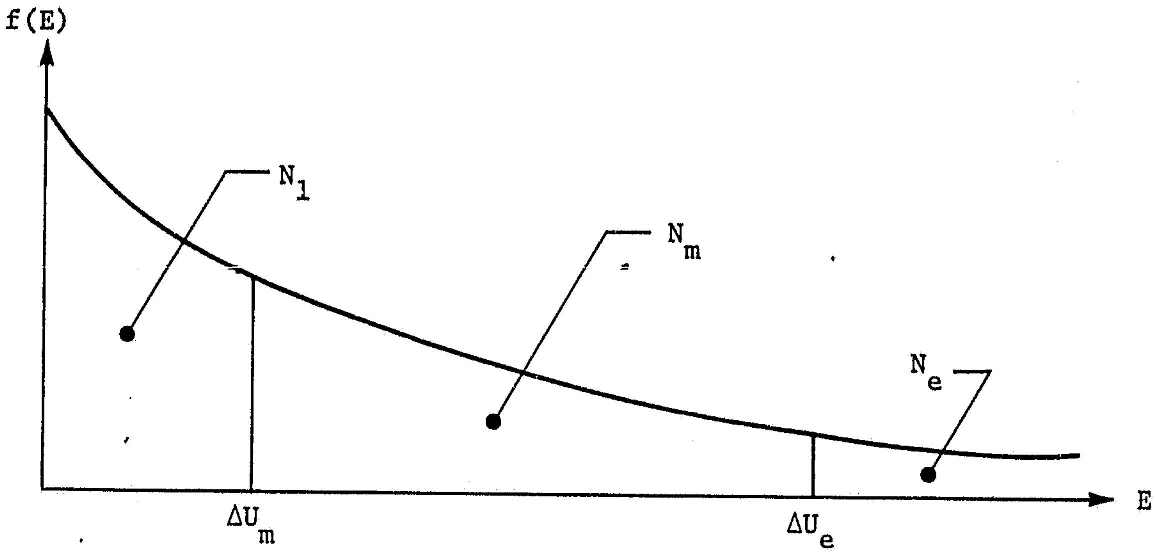

Figure 5. Boltzmann distribution.

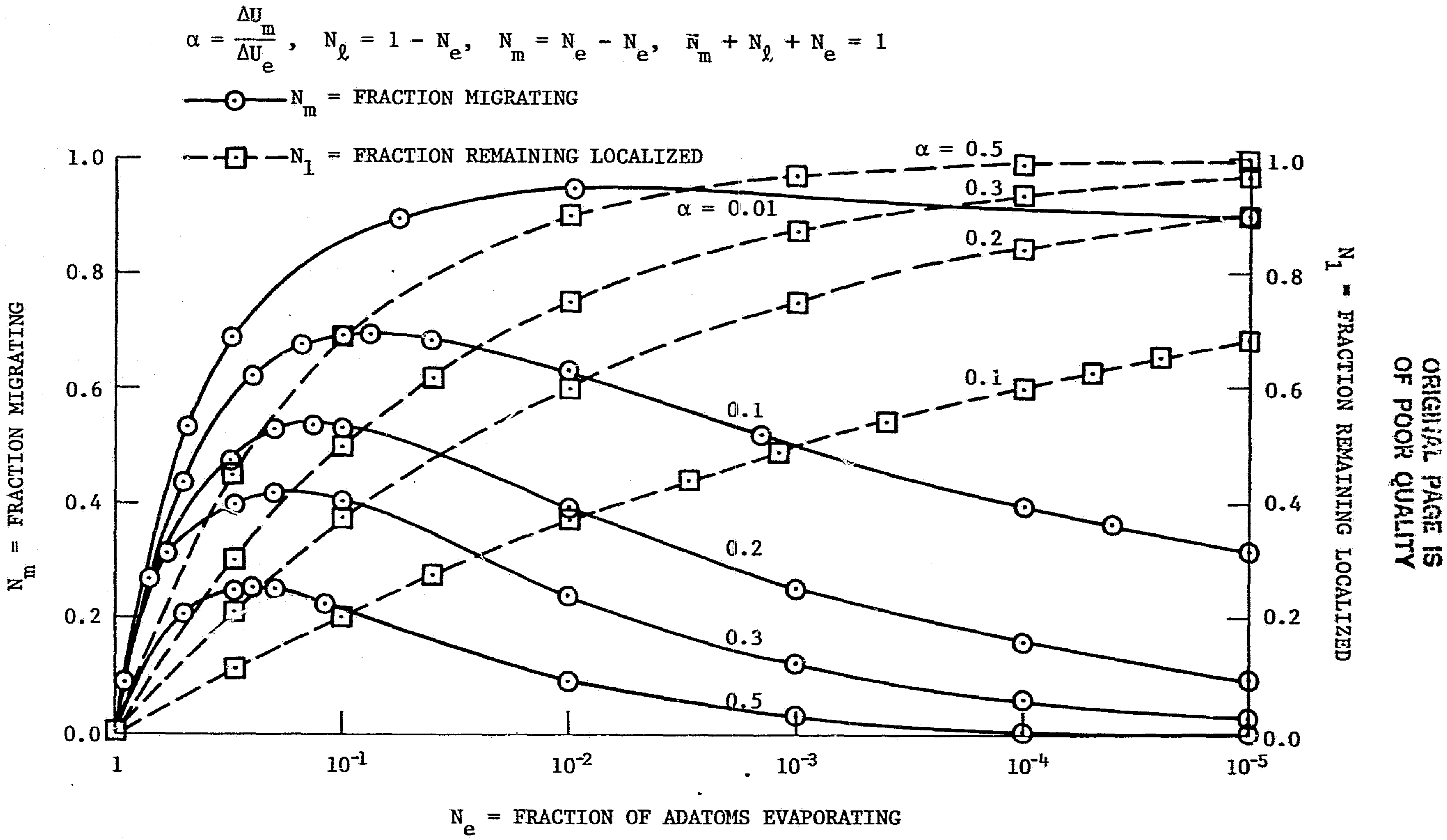

Figure 6. Evaporation, migration, and localization of adatoms for various values of $\Delta U_m/\Delta V_e$.

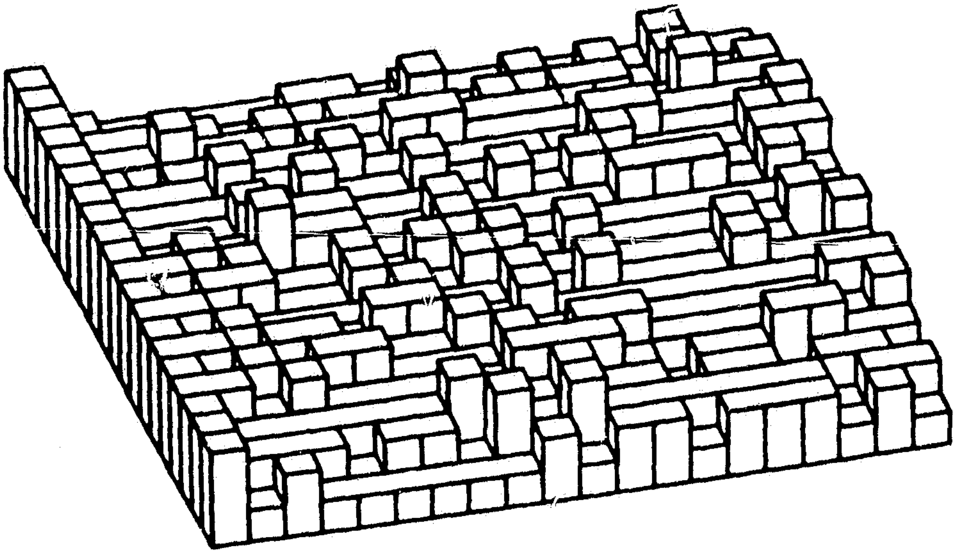

Figure 7. Graphic display of crystal growth (100) orientation.